Liver Iron Concentration Evaluated by Two Magnetic Methods: Magnetic Resonance Imaging and Magnetic Susceptometry

Antonio Adilton O. Carneiro,[1]* Juliana P. Fernandes,[1] Draulio B. de Araujo,[1] Jorge Elias Jr.,[2] Ana L. C. Martinelli,[2] Dimas T. Covas,[2] Marco A. Zago,[2] Ivan L. Ângulo,[3] Timothy. G. St. Pierre,[4] and Oswaldo Baffa[1]

Quantification of liver iron concentration (LIC) is crucial in the management of patients suffering from certain pathologies that can produce iron overload, such as Cooley's anemia and hemochromatosis. All of these patients must control the level of iron deposits in their organs to avoid the toxicity of high LIC, which is potentially lethal. This paper describes experimental protocols for LIC measurement using two magnetic techniques: magnetic resonance imaging (MRI) and biomagnetic liver susceptometry (BLS). MRI proton transverse relaxation rate (R_2) and image intensity, evaluated pixel by pixel, were used as indicators of iron load in the tissue. LIC measurement by BLS was performed using an AC superconducting susceptometer system. A group of 23 patients with a large range of iron overload (0.9 to 34.5 mgFe/$g_{dry\ tissue}$) was evaluated with both techniques (MRI × BLS). A significant linear correlation (r = 0.89–0.95) was found between the LIC by MRI and by BLS. These results show the feasibility of using two noninvasive methodologies to evaluate liver iron store in a large concentration range. Both methodologies represent an equivalent precision. Magn Reson Med 54:122–128, 2005. © 2005 Wiley-Liss, Inc.

Key words: liver iron; Cooley's anemia; hemochromatosis; magnetic resonance imaging; magnetic susceptometry; SQUID

Iron is an essential element in all living cells, but becomes toxic if accumulated beyond the capacity of its storage proteins (ferritin and hemosiderin) and its transport protein (transferin). Iron overload causes damage to the liver, various endocrine organs, and the heart (1–4). This condition may result from increased gastrointestinal absorption or from repeated blood transfusions (5–7), when chronically transfused and inadequately chelated patients develop cellular injury, skin hyperpigmentation, and growth retardation. This is followed in adolescence by pubertal failure, insulin-dependent diabetes, hypothyroidism, cardiac failure, and arrhythmias (8,9). Practical management of iron overload requires a reliable estimation of body iron content and its distribution, as well as an understanding of how iron overload produces clinical sequelae (10).

The safest and most effective way of removing iron excess depends on the underlying condition as well as on the degree of iron load. Therefore, the use of noninvasive techniques to serially evaluate body iron overload is very useful to monitor the efficacy of the treatment (11).

In the majority of clinical centers, the standard method to evaluate the total amount of body iron is measurement of the serum ferritin concentration in the blood. However, the correlation between serum ferritin and body iron is not sufficiently precise to be of strong prognostic value, especially in association with inflammation or tissue damage (12). Moreover, the relationship between blood serum ferritin concentration and body iron content is altered in a complex manner by chelation and vitamin C treatment. In addition, the relationship between serum ferritin and body iron appears to be different for different hematologic conditions (9,13).

An alternative to evaluating body iron overload is the measurement of liver iron concentration (LIC). Liver is the main iron storage in the body, containing approximately 70% of the total content (14). Liver iron correlates closely with total body iron and can be assessed by needle biopsy or, more recently, by noninvasive magnetic resonance imaging (MRI) and biomagnetic liver susceptometry (BLS).

Needle biopsy is the current gold standard technique, which can provide direct LIC measurement by atomic absorption spectroscopy and histologic evolution of the liver pathology. However, liver biopsy cannot be used as a routine method due to its invasiveness, discomfort, and significant risk to the patient. In addition, inadequate sample size (<0.5 mg dry weight) and nonuniform liver iron distribution may give misleading results (15).

On the other hand, MRI has recently proved its effectiveness in measuring LIC (16). The presence of iron ions in a sample causes a reduction of MRI signal intensity, which is related to a decrease in T_2 relaxation time of the protons (17). Based on this principle, MRI may serve as a noninvasive technique to determine LIC (18–23). Recent studies have shown that the logarithm of signal intensity (SI) and transverse relation rate R_2 (= $1/T_2$) of images acquired using gradient-echo and spin-echo sequences have a linear correlation with needle biopsy (24–27). Nevertheless, MRI measurements in patients with severe iron overload are inaccurate due to ultrafast transverse relaxation times. Thus, there is an upper limit of LIC that can be evaluated by MRI (28). Another disadvantage of MRI is its

[1]Departamento de Física e Matemática, FFCLRP, Universidade de São Paulo, Ribeirão Preto, São Paulo, Brazil.

[2]Departamento de Clínica Médica, FMRP, Universidade de São Paulo, Ribeirão Preto, São Paulo, Brazil.

[3]Centro Regional de Hemoterapia, HCFMRP, Universidade de São Paulo, Ribeirão Preto, São Paulo, Brazil.

[4]Department of Physics, University of Western Australia, Nedlands, Western Australia, Australia.

Grant sponsors: Brazilian agencies FAPESP, CNPq, and CAPES.

*Correspondence to: Antonio Adilton Carneiro, Departamento de Física e Matemática, FFCLRP-USP, Av. Bandeirantes, 3900, 14040–901 Ribeirão Preto-SP, Brazil. E-mail: adilton@biomag.usp.br

Received 25 October 2004; accepted 20 January 2005.

DOI 10.1002/mrm.20510
Published online in Wiley InterScience (www.interscience.wiley.com).

dependence on tissue alterations such as fibrosis and inflammation, which are common in patients with iron overload (13). However, MRI has the advantage of allowing assessment of iron load in different storage organs, such as the heart and the spleen.

Another technique capable of determining LIC is BLS, which is the most specific noninvasive method of estimating LIC. BLS is a direct method that is able to quantify LIC at levels from normal (0.05 LIC $<$ 0.50 mg Fe/g_{liver}) to overloads up to 8 mg Fe/g_{liver}. It uses a magnetic susceptometer based on the superconducting quantum interference device (SQUID) detector (29–32). The susceptometric technique entails measurement of magnetic field variations produced in the region of the liver in response to an external magnetizing field. Normal tissue is diamagnetic and has a magnetic susceptibility (χ) close to that of water (-9.032×10^{-6} S.I. When iron atoms are present, χ is modified and the variation of the magnetization is proportional to the amount of iron present. Therefore, iron load alters the signal measured by the susceptometer.

The response of the susceptometer is dependent on the geometry of the magnetizing and detection coils, the size of the sample, and the sensor-to-sample distance (33). Therefore, in LIC evaluation, the sensor-to-skin distance and the liver depth should be precisely measured. To minimize the influence of different tissues (skin, fat, bone, etc.), a water bag is placed around the torso, homogenizing the geometry. The measurement is performed with the patient in a supine position on a nonmagnetic bed below the magnetic detector. Other parameters like radius of the upper curvature of the torso, height, weight, and age were also recorded for use in the mathematical model applied to calculate LIC. The computed variation of magnetization is linearly proportional to LIC.

In this paper we compare the results of LIC as obtained by MRI and BLS in the same group of patients and evaluate their correlation with serum ferritin measurements. Also, two different MRI modalities to infer iron overload, based on spin echo (SE) and gradient echo (GRE) acquisitions, is compared. The relationship between the liver iron concentration and signal intensity was evaluated for all images acquired by SE and GRE sequences.

METHODS

Patients

A group of 27 patients was studied (23 men, 4 women; age range, 7–68 years old; mean age, 30 years old). Thirteen had chronic anemia and received blood transfusions regularly, 1 had hemochromatosis, and 13 had hepatitis C. Of this group 4 were claustrophobic and could not be evaluated by MRI. The Ethics Committee of the Hospital and Clinics of Faculdade de Medicina de Ribeirao Preto approved the study protocol and informed consent was obtained from all patients.

Biomagnetic Liver Susceptometry

BLS measurement was performed using a susceptometer based on a RF-SQUID. This system applied a homogenous (~5 ppm) AC magnetizing field (114 μT and 7.7 Hz) in the hepatic region. The detector consisted of a second-order gradiometer coil with diameter 2.5 cm and baseline 4 cm. A water bag of approximate volume 5 L surrounded the torso in order to minimize other tissue contributions. A special vacuum mattress fixed the subject in a comfortable position and also supported the water bag. A simplified drawing of the biomagnetic susceptometer system and the patient position is presented in Fig. 1.

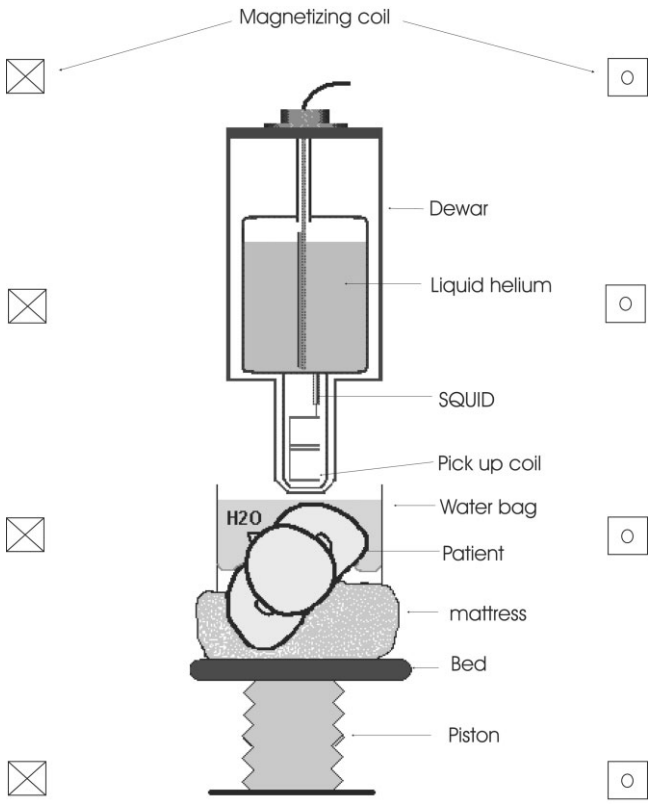

FIG. 1. Simplified diagram of the susceptibility system apparatus showing the superconducting detector coil immersed in liquid helium, positioning of the patient, the water bag, and the magnetizing coil distribution around the patient.

To evaluate the depth and size of the liver and the distance between the liver and the lung we used an ultrasound scanner (Hitachi EUB-305), with the patients lying in position for the susceptometric measurements (supine position with the body rotated about 35° relative to the vertical axis).

To perform BLS measurements, the bed was moved down 8 cm at a constant speed of 2 mm/s. The liver iron concentration, corresponding to the variation of the magnetization detected, was calculated with software developed using Matlab 6.5 (Mathworks Inc., Natick, MA, USA). The algorithm takes into account all of the factors mentioned above in estimating the LIC; all of the various tissue susceptibilities are considered, especially those of the lungs.

In this susceptometer configuration, the output signal is practically zero when a measurement is performed in a large volume, like an adult torso, with homogenous susceptibility. Thus, in the measurements reported here, the output signal is generated mainly by the iron distributed in the liver volume.

Since the magnetizing field is homogenous over the entire torso, a large volume near the sensor also contributes to the susceptometric measurement. The main contribution of the lung is related to the absence of tissue in the air cavities. The mean volume susceptibility of the biologic tissue (χ_{tissue}) is practically equal to that of water ($\sim 9.03 \times 10^{-6}$ S.I.) and the air volume susceptibility (χ_{air}) is equal to 0.36×10^{-6} S.I.. Therefore, the lungs have an effective susceptibility equal to $\chi_{tissue} - \chi_{air} = 9.39 \times 10^{-6}$ S.I. The iron concentration corresponding to this lung contribution is approximately 2 mg Fe/$g_{wet\ tissue}$ (32). Due to their small volume and large distance from the center of the liver, other neighboring organs with different susceptibility, such as the heart and spleen, give a negligible contribution for this susceptometer configuration (33). The volume susceptibility ($\Delta\chi$) of iron in the liver is given by the product of the LIC and the mass susceptibility of hepatic iron ($\chi_{m,ftn} = 1.6 \times 10^{-6}$ m^3/kg) (34).

The LIC is calculated from the signal output of the BLS, based on modeling of the magnetic flux assuming a spherical and cylindrical geometry for the liver and lung, respectively, using the equation

$$LIC = \frac{1}{\chi_{m,ftn}\Delta\Sigma_{liver}}\left[\frac{\mu_0(\Delta V_{BLS} - \Delta V_{system} + \delta)}{C} - (\chi_{air} - \chi_{tissue})\,\Delta\sum_{lung}\right], \quad [1]$$

where ΔV_{system} is the system (bed, bag, etc.) contribution expressed as the output voltage of the sensor, measured keeping the same position and displacement of the bed, but without the patient; δ is a correction factor to compensate for the small difference in the signal caused mainly by the susceptibility mismatch between the water in the bag and hepatic tissue; C is the calibration factor; μ_0 is the vacuum permeability; and $\Delta\Sigma$ is the variation of the integral volume (see equation below) calculated over the liver and lung volume when the torso is displaced. The integral is given by

$$\Sigma_{vol} = \int_{vol} \bar{B}_m(r) \cdot \frac{\bar{B}_d(r)}{I_d}\, d^3r, \quad [2]$$

where $\bar{B}_m(\bar{r})$is the magnetizing field density and $\bar{B}_d(\bar{r})$ is the magnetic field density that the detector coils would generate in the element of volume (d^3r) if energized with a current I_d.

The calibration factor C is intrinsic to the susceptometric system and was obtained from measurements on a cylindrical phantom, with dimensions equivalent to an adult human torso filled with pure water. The factor δ was determined from measurements in a control group of 34 normal volunteers (32). In this case, an average liver iron store of 0.20 mg Fe/g_{liver} in the normal volunteers was assumed (30) and the average value of δ was calculated using Eq. [1]. As the water content in hepatic tissue is about 71%, the output of the BLS results was multiplied by a factor of 3.45 for conversion to concentration referred to dry tissue weight.

MRI Procedure

To evaluate liver iron overload, MR images were acquired using two SE and two GRE sequences on a 1.5-T whole-body scanner (Siemens Magneton Vision Plus). The first SE sequence was a multislice single-spin-echo (SSE) sequence (TR = 2500 ms, matrix = 192 × 256, TE = 6, 7, 8, 9, 12, 15, and 18 ms, and slice thickness = 5 mm). The seven repeated sequences were acquired under fixed signal amplifier gain, lasting 4 min each. This SSE sequence was developed by Clark and St. Pierre (27) to evaluate liver iron overload using proton transverse relaxation rates. The second SE sequence was a single-slice multi-spin-echo (MSE) sequence (TR = 2000 ms, matrix 256 × 256, TE = 22.5, 45, and 300 ms, and slice thickness = 8 mm), lasting approximately 5 min.

A saline solution bag was used as a reference in all MRI measurements. It had a volume of 1 L and was placed at the left side of the torso. The SE sequences were employed without attempting to use respiratory gating or breath-holding techniques.

As TR is large compared to typical T_2 and T_1 relaxation times of the liver tissue, the transverse relaxation rate, R_2, was calculated by fitting the image signal intensities by the exponential equation (25,27)

$$S_{SE}(TE) = S_{SE}(0)e^{-R_2 TE} + S_{LO}, \quad [3]$$

where S_{LO} is the signal level offset and S_{SE} (0) is the signal intensity at TE = 0 ms.

The transverse relaxation rate, R_2, was evaluated pixel by pixel on a selected region of interest (ROI), and a histogram was used to assess R2 distribution. A set of Gaussian functions was fitted to the R_2 distribution and the weighted average value of the distribution that corresponds to the hepatic tissue was used as the R_2 value (Fig. 2) (35). Fluctuations in voxel intensity, caused mainly by respiratory motion, were filtered using a 5 × 5 smoothing window, progressively centered on each voxel in the ROI. Variations of liver signal intensity (SI_{liver}) between the images acquired with different TE were corrected using the signal intensity of the water bag imaged together with the patient ($SI_{water\ bag}$). For the pulse parameters used, it was expected that the signal intensity coming from the water in the saline would have almost same intensity for all TE.

LIC values from relaxometry (R_2) using SSE sequences were computed according to the protocol developed by Clark and St. Pierre (27), who have validated their protocol of quantifying iron overload from R_2 with more than 100 biopsies (37). To evaluate possible image differences caused by homogeneity of the magnetic field between our scanners, a phantom with paramagnetic material that produces a disturbance in the proton relaxation equivalent to that caused by the iron levels found in the human liver tissue was imaged in our scanner and at the scanner used by Clark and St. Pierre with the same protocol used in the patients. Therefore, any differences in the R_2 of the phantom could be used to correct the R_2 in the patients.

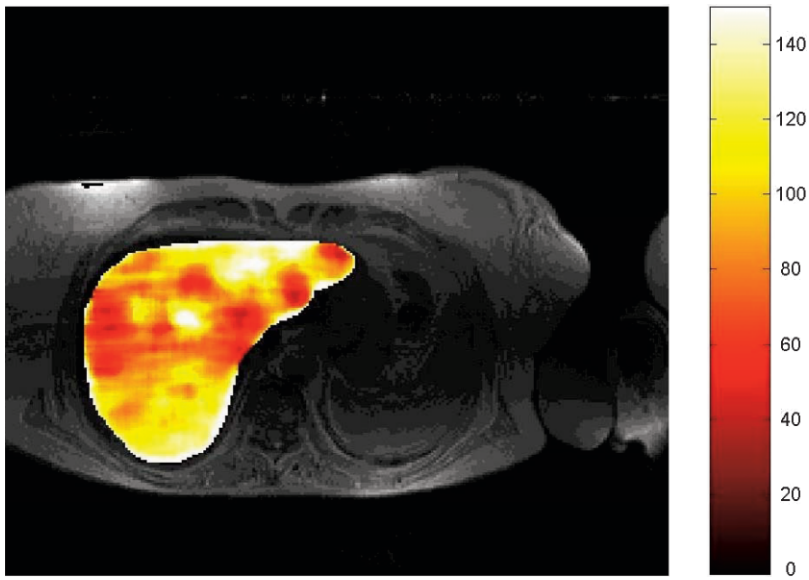

FIG. 2. Transverse relaxation rate (R_2) map of the liver superimposed on the 6-ms spin-echo image. Bright areas indicate high relaxation values, suggesting high iron concentration. The scale at right of the figure represents the R_2 value on the liver region. High R_2 values indicate high LIC regions.

The GRE sequences (TR = 18 ms, TE = 5 ms, flip angles = 10 and 70° and slice thickness = 8 mm) were performed with breath holding using a single section with a 256 × 128 matrix. These GRE sequences were chosen based on the methodology presented by Bonkovsky et al. (24). The imaged slice was on the middle of the upper lobule of the liver and the ratio of the signal intensity in the liver region to the background signal was evaluated. The average pixel intensity in a ROI, covering the entire liver but avoiding veins and arteries, was used. The background signal was taken from a region outside the torso and free of breathing artifacts.

RESULTS

The iron evaluation by the three different methodologies (serum ferritin, MRI, and BLS) was performed in a time interval shorter than 15 days for the same patient. The LIC values for the 27 patients evaluated by BLS varied from 0.9 to 34.5 mg $Fe/g_{dry\ tissue}$ (mean LIC ± SD = 12.1 ± 9.9 mg $Fe/g_{dry\ tissue}$).

The correlation coefficient between serum ferritin and LIC deduced by BLS was 77% (Fig. 3). This relatively low correlation was expected since serum ferritin is not a good parameter to evaluate total body iron.

Table 1 shows the correlation among all MRI analyses and the BLS results. As shown in Fig. 4, the LIC measured by the relaxometric protocol using the SSE sequence, versus LIC measured by BLS, showed a correlation of 93%. The same high correlation was observed between the logarithm of the liver-to-background signal intensity ratio for TE of 15 ms and the BLS results.

The relaxation rate (R_2) evaluated from the MSE sequence showed a low correlation (63%) with BLS. Figure 5 shows the logarithm of the liver-to-background signal intensity ratio from the MSE sequence versus the BLS results. In this case a correlation 95% was found.

Figure 6a and b shows MRI results using GRE sequences versus BLS results. As found by Bonkovsky et al. (24) the GRE sequence showed a higher correlation for flip angle 10° (91%) than for flip angle 70° (89%), as shown in Fig. 6.

This high correlation of MRI with BLS is similar to the results of MRI versus LIC by biopsy presented by other authors (23–25).

DISCUSSION

By the first time, the two most precise and specific noninvasive methods available to evaluate liver iron concentration were applied to patients with liver iron overload. The biomagnetic liver susceptometry measurement, performed with a biosusceptomer developed in our laboratory (34), demonstrated high efficacy and specificity in liver iron quantification. In addition, the procedure is well tolerated by patients, an important issue for pediatric and claustrophobic patients. The total time of BLS measurement was about 20 min, including all three acquisitions that were performed in each session.

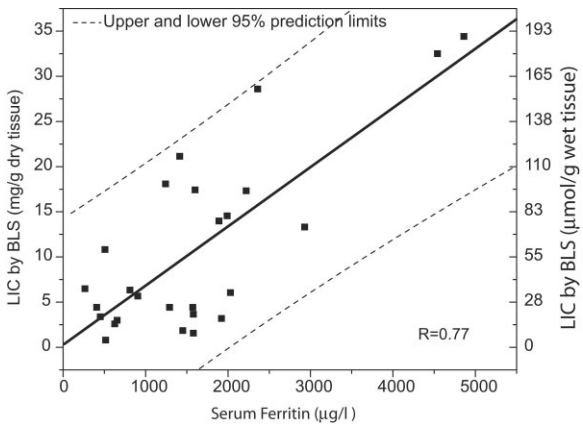

FIG. 3. Correlation between LIC by BLS and serum ferritin for 27 patients with iron overload. A 77% of correlation was obtained.

Table 1
MR Imaging Sequences Evaluated

Sequence (parameter measured)	TR/TE (ms)	Correlation MRI × BLS (*r* values, %)
SSE (R_2)	2500/(6,7,8,9,12,15,18)	+93
SSE (SI)	2500/6	−77
SSE(SI)	2500/9	−83
SSE (SI)	2500/12	−89
SSE (SI)	2500/15	−93
SSE (SI)	2500/18	−90
MSE (SI, first echo)	2000/22.5	−95
GRE (SI)	18/5, fa = 10°	−91
GRE (SI)	18/5, fa = 70°	−89

Note. R_2, transversal relaxation rate ($1/T_2$); SI, signal intensity; fa, flip angle.

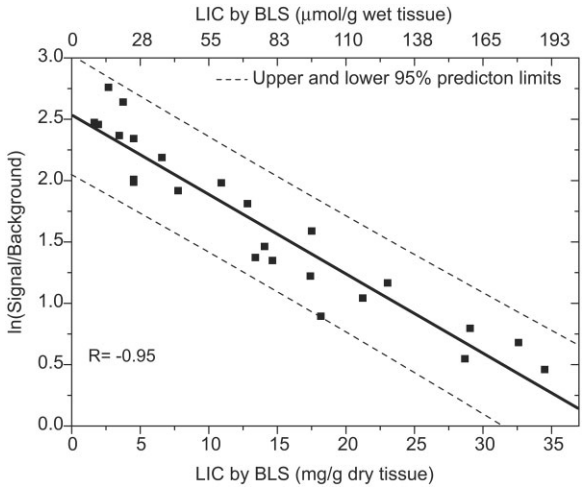

FIG. 5. Results of the MRI analysis acquired by MSE sequence versus LIC obtained by BLS. MRI signal was analyzed by the mean value of the intensity signal of each pixel of the ROIs. The image shown was acquired with TE of 22.5 ms.

The SE and GRE sequences used in this study to acquire MR images were similar to the ones used by other authors (24,27), and the high correlation found in this work between LIC measured by MRI and by BLS was consistent with the high correlation found by these authors between MRI and needle biopsy. Figures 5 and 6 show clearly that, using standard sequences currently available in most clinical centers, the GRE sequence with (TR/TE/FA = 18/5/10° or 70°) is not able to assess LICs higher than 30 mg Fe/g $_{\text{dry tissue}}$.

The relaxometry method using a long TR and a short TE was able to evaluate LICs as high as 40 mg Fe/$g_{\text{dry tissue}}$, as indicated by Clark and St. Pierre (27). This LIC value corresponds to a very high iron load in regularly transfused patient. Generally, most carefully chelated patients have a LIC less than 40 mg Fe/$g_{\text{dry tissue}}$.

In our results, the MRI parameter that best correlated with the BLS results was the signal intensity of the first echo of the MSE sequence. This sequence was used to evaluate the transversal relaxation, R_2. But the very low signal intensity in the liver region, already by the second echo, even for low LIC, was responsible for the low correlation between R_2 and BLS (63%).

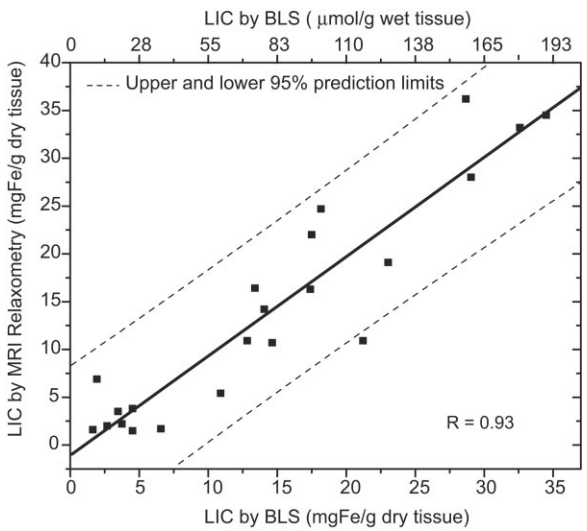

FIG. 4. LIC by transverse relaxation of MRI imaging using SSE sequence versus LIC by BLS.

Bonkvosky et al. (24) found a low correlation of the MRI signal intensity using a SE (TR = 2000 ms and TE = 12 and 80 ms) sequence with LIC by biopsy. Upon analyzing the SI of images acquired with the SSE sequence for all TE (Table 1), we found that its correlation with LIC by BLS is lower for TE values shorter than the T_2 value of the liver tissue. The correlation increased when TE was closer to the mean T_2 value. A possible explanation could be the very long TR and very short TE, compared with transverse relaxation time (T_2) of the target tissue. In this situation, the SI is proton density weighted; consequently, it is more sensitive to such tissue conditions as fibrosis. On the other hand, if the TE is larger than T_2 of the tissue, the SI is T_2-weighted and will be close to the background noise SI. The T_2 value in normal liver is approximately 40 ms and in patients with moderate LIC the typical value of T_2 is about 20 ms.

One difficulty in using MRI to evaluate LIC is variation of control parameters and magnetic field inhomogeneity between different scanners. This can be overcome by calibrating the scanner with a standard phantom and using this same reference phantom together with the patient as was indicated by Pierre et al. (37) This procedure of calibration was employed in this work.

This work confirms the feasibility of using two noninvasive methodologies to quantify liver iron concentration at levels from normal to the highest found in common clinical practice. These techniques have potential application in guiding therapy to control the liver iron balance in patients submitted to blood transfusion and iron chelation treatment and in evaluating the efficacy of new oral chelation agents. Although both techniques, MRI and BLS, are able to evaluate a wide range of LIC in vivo, some important comments should be made. BLS is presented in the literature as a direct and more precise noninvasive methodology. The precision of the measurement is related to the physical model that involves

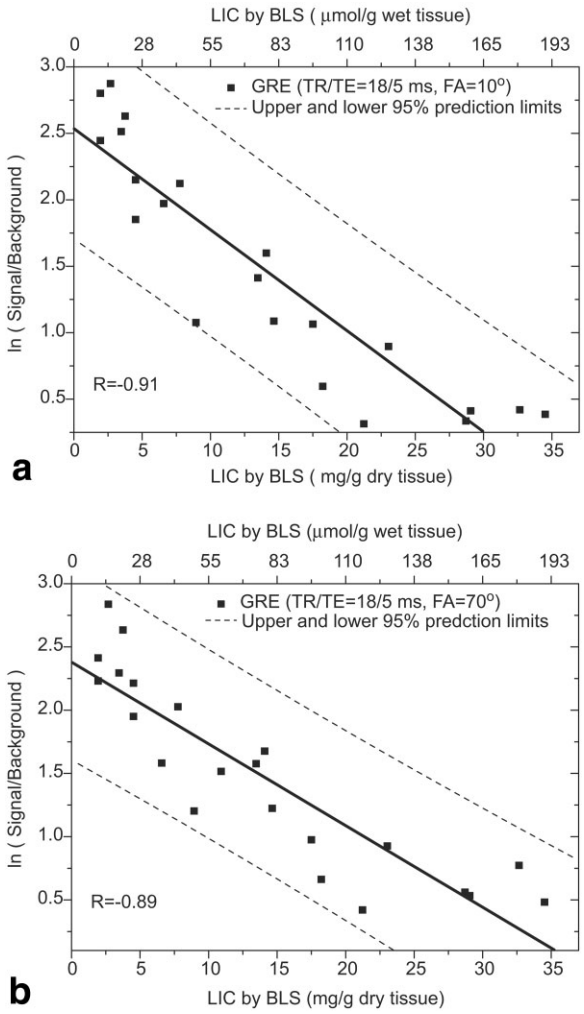

FIG. 6. Results of the MRI analysis acquired by GRE sequence with (**a**) flip angle = 10° and (**b**) flip angle = 70° versus LIC by BLS.

the geometric modeling of each torso. In addition, BLS measurement is very sensitive to the position of the patient and in particular to the susceptometer-skin distance (33). If this parameter is carefully controlled, BLS becomes a useful tool to follow variations of iron store in patients regularly transfused with the body iron balance controlled by chelation therapy.

In contrast to BLS, MRI signal intensity decreases with increasing iron stores and is affected by tissue damage. But with the development of improved protocols for acquisition and imaging processing, this uncertainty has been minimized (27,35,36). An important advantage of MRI over BLS is its potential to evaluate iron distribution throughout the organ and to show it as image contrast. The MRI protocol is well suited to a clinic with a small number of patients that already has an MRI scanner.

In conclusion, the high correlation found between the LIC by BLS and the LIC by MRI suggests that the present state-of-the-art MRI systems and pulse sequences can be calibrated with phantoms to perform accurate LIC.

REFERENCES

1. Olivieri NF, Nathan DG, MacMillian JH, Wayne AS, Liu PP, McGee A, Martin M, Koren G Cohen AR. Survival in medically treated patients with homozygous beta-thalassemia. N Engl J Med 1994;331:574–578.
2. Modell B, Khan M, Darlison M. Survival in beta-thalassemia major in the UK. Lancet 2000;355:2051–2052.
3. Aldouri MAWB, Hoffbrand AV, Flynn DM, Ward SE, Agnew JE, Hilson AJ. High incidence of cardiomyopathy in beta thalassemia patients receiving regular transfusion and iron chelation. Acta Haematol 1990; 84:113–117.
4. Ballas SK. Iron overload is a determination of morbidity and mortality in adult patients with sickle cell disease. Semin Hematol 2001;38:30–36.
5. Olivieri NF. Progression of iron overload in sickle cell disease. Semin Hematol 2001;38:57–62.
6. Brittenham GM, Cohen AR, Mclaren CE, Martin MB, Griffith PM, Nienhuis AW, Young NS, Allen CJ, Farrell DE, Harris JW. Hepatic iron stores and plasma ferritin concentration in patients with sickle cell anemia and thalassemia Major. Am J Hematol 1993;42:81–85.
7. Niederau C, Fischer R, Pürschel A, Stremmel W, Haüssinger D, Strohmyeyer G. Long-term survival in patients with hereditary hemochromatosis. Liver, pancreas, and biliary tract. Gastroenterology 1996;110: 1107–1119.
8. Fosburg MT, Nathan DG. Treatment of Cooley's anemia. Blood 1990; 76:435–444.
9. Davis BA, Porter JB. Long-term outcome of continuous 24-hour deferoxamine infusion via indwelling intravenous catheters in high-risk beta-thalassemia. Blood 2000;95:1229–1236.
10. Brittenham GM, Sheth S, Allen CJ, Farrel DE. Noninvasive methods for quantitative assessment of transfusional iron overload in sickle cell disease. Semin Hematol 2001;38:37–56.
11. Porter JB. Practical management of iron overlad. Br J Hematol 2001; 115:239–252.
12. Nielsen P, Gunther V, Dyrken M. Serum ferritin iron in iron overload and liver damage: correlation to body iron stores and diagnostic relevance. J Lab Clin Med 2000;135:413–418.
13. Angelucci E, Muretto PO, Nicolucci A, Baronciani D, Erer B, Gazlev J, Ripati M, Sodani P, Tomassoni S, Visane G, Lucarel G. Effects of iron overload and hepatitis C virus positivity in determining progression of liver fibrosis in thalassemia following bone marrow transplantation. Blood 2002;100:17–21.
14. Angelucci E, Brittenham GM, McLaren CE, Ripalti M, Baronciani D, Giardini C, Galimberti M, Polchi P, Lucarelli G. Hepatic iron concentration and total body iron stores in thalassemia major. N Engl J Med 3431:2000.
15. Villeneuve JP, Bilodeau M, Lepage R, Cote J, Lefebvre M. Variability in hepatic iron concentration measurement from needle-biopsy specimens. J Hepatol 1996;25:172–177.
16. Koenig SH, Brown RD III, Gibson JF, Ward RJ, Peters TJ. Relaxametry of ferritin solutions and the influence of the Fe^{3+} core ions. Magn Reson Med 1986;3:755–767.
17. Baffa O, Tannus A, Zago MA, Figueiredo MS, Panepucci HC. Changes in NMR relaxation times of iron overloaded mouse tissue. Bull Magn Reson 1986;8:69–73.
18. Gomori J, Horev G, Tamary H, Zandback J, Kornereich L, Zaizov R, Freus E, Krief O, Bem-Meir J, Rotem H, Kuspet M, Rosen P, Rachamilewitz EA, Loewenthal E, Gorodetsky. Hepatic iron overload: quantitative MR imaging. Radiology 1991;179:367–368.
19. Engelhardt R, Langkowski JH, Fischer R, Nielsen P, Kooijman H, Heinrich HC, Bücheler E. Liver iron quantification: studies in aqueous iron solutions, iron overloaded rats and patients with hereditary hemochromatosis. Magn Reson Imaging 1994;12:999–1007.
20. Dixon RM, Styles P, Al-Refaire FN, Kemp GJ, Donohue SM, Wonke B, Hoffbrand AV, Radda GK, Rajagoplan B. Assessement of hepatic iron overload in thalassemic patients by magnetic resonance spectroscopy. Hepatology 1994;19:904–910.
21. Thomsen C, Wiggers P, Ring-Larsen H, Christiansen E, Dalhoj J, Henriksen O, Christoffersen P. Identification of patients with hereditary haemochromatosis by magnetic resonance imaging and spectroscopic relaxation time measurements. Magn Reson Imaging 1992;10:867–879.
22. Kaltvasser JP, Gottschalk R, Schalk KP, Hartl W. Non-invasive quantification of liver iron-overload by magnetic resonance imaging. Br J Haematol 1990;74:360–363.

23. Jensen PD, Jensen FT, Christensen T, Ellergaard J. Non-invasive assessment of tissue iron overload in the liver by magnetic resonance imaging. Br J Haematol 1994;87:171–184.
24. Bonkovsky HL, Rubin RB, Cable EE. Hepatic iron concentration: noninvasive estimation by means of MR imaging techniques. Radiology 1999;212:227–234.
25. Papakonstatinou O, Kostaridou S, Maris T, Gouliamos A, Premetis E, Kouloulias V, Nakopoulou L, Kattamis C. Quantification of liver iron overload by T2 quantitative magnetic resonance imaging in thalassemia: impact of chronic hepatitis C on measurements. J Pediatr Hematol/Oncol 1999;21:142–148.
26. Kreeftenberg Jr. HG, Mooyaart EL, Huizenga JR, Sluiter WJ, Kreeftenberg HG. Quantification of liver iron concentration with magnetic resonance imaging by combining T1, T2- weighted spin echo sequences and a gradient echo sequence. Netherlands J Med 2000;56:133–137.
27. Clark PR, St. Pierre TG. Quantitative mapping of transverse relaxivity ($1/T_2$) in hepatic iron overload: a single spin-echo imaging methodology. Magn Reson Imaging 2000;18:431–438.
28. Pardoe H, Chua-anusorn W, St. Pierre TG, Dobson J. Detection limits for ferromagnetic particle concentrations using resonance imaging based proton transverse relaxation rate measurements. Phys Med Biol 2003; 8:N89–N95.
29. Pasquarelli A, Del Gratta C, Della Penna S, Di Luzio S, Pizzella V. A SQUID based AC susceptometer for the investigation of large samples. Phys Med Biol 1996;41:2533–2539.
30. Paulson DN, Fagaly RL, Toussaint RM. Biomagnetic susceptometer with SQUID instrumentation. IEEE Trans Magn 1990;27:3249–3252.
31. Wikswo JP, Fairbank Jr. WM, Opfer JE. Method for measuring externally of the human body magnetic susceptibility changes, United States Patent 1976;3:980,076.
32. Carneiro AAO, Fernandes JP, Zago MA, Covas DT, Angulo IL, Baffa O. AC superconductor susceptometric system to evaluate liver iron overload. Rev Sci Instrum 2003;74:3098–3103.
33. Carneiro AAO, Baffa O, Fernandes JP, Zago MA. Theoretical evaluation of the susceptometric measurement of iron in human liver by four different susceptometers. Physiol Meas 2002;23:683–693
34. Andrã W & Nowak H. Liver iron susceptomtry. In: Magnetism in medicine; Wiley-VCH: Berlin, 1998. p 286–301.
35. Clark PR, Chua-anusorn W, St Pierre TG. Reduction of respiratory motion in transverse relaxation rate (R2) images of the liver. Comput Med Imaging Graph 2004;28:69–76.
36. Clark PR, Chua-anusorn W, St Pierre TG. Proton transverse relaxation rate (R-2) images of iron-loaded liver tissuepping local tissue iron concentrations with MRI. Magn Reson Med 2003;49:572–575.
37. Pierre TG St., Clark PR, Chua-anusorn W, Fleming AJ, Jeffrey GP, Olynyk JK, Pootrakul P, Robins E, Lindeman R. Noninvasive measurement and imaging of liver iron concentrations using proton magnetic resonance. Blood, published online July 15, 2004.